

Ultraviolet-photoemission studies of TlCl†

S. F. Lin and W. E. Spicer

Stanford Electronics Laboratories, Stanford University, Stanford, California 94305

(Received 9 December 1974)

In-situ-prepared TlCl films have been studied with photoemission for photon energies up to 11.8 eV. Photoelectron energy-distribution curves (EDC's) show two strong valence-band density of states at 1.0 and 2.2 eV below the valence-band maximum (VBM) and one weaker piece of structure at 3.4 eV below the VBM. They also suggest a strong conduction-band density of states near 8.1 eV and a minimal density-of-states region 9.0–10.0 eV above the VBM. The valence-band width estimated from the EDC's is 4.0 eV. Comparing these features to theoretical calculations, the relativistic Korringa-Kohn-Rostoker calculation by Overhof and Treusch yields correct valence-band width and gives fair qualitative but not quantitative agreement. The electron escape length for electrons 6.9 to 7.6 eV above the VBM (0–0.7 eV above the photoelectric threshold) is estimated to be 200 Å by photoinjection method. EDC's also exhibit strong temperature dependence. It is suggested that this is due to the dynamic modulation of the orbital hybridization in the valence-band electronic states because of lattice vibrations. It is further suggested that the effect of lattice vibrations on electrons (or vice versa) cannot be treated as a perturbation in the usual electron-phonon interaction approach, and may be responsible for unusual lattice dynamics of TlCl. Exposure of TlCl thin films to Cl₂ gas up to 500 langmuirs (at 1×10^{-8} Torr) at 25 and 50°C yielded no change of EDC's.

I. INTRODUCTION

Over the last decade extensive studies have been made on strongly ionic alkali halides and mostly covalent semiconductors. The basic properties of these materials thus have been very well understood and are playing important roles in the utilization of these materials. Thallous halides, on the other hand, being ionic with somewhat covalent nature,¹ have not been understood to such an extent.

However, during the past few years, a considerable amount of effort has been made in trying to understand the basic properties of these materials by means of techniques such as cyclotron-resonance measurements,^{2,3} two-photon absorption measurement,^{4,5} magneto-optical absorption measurements,^{6,7} soft-x-ray absorption,^{8–10} and emission¹¹ experiments, optical absorption measurements,^{12–14} and inelastic-neutron-scattering experiments,¹⁵ etc. Through these efforts, properties of thallous halides have become considerably clearer. All these make uv-photoemission studies on these materials timely.

The outer configurations of Tl⁺ and Cl[−] are, respectively, $4f^{14}5d^{10}6s^2$, and $3s^23p^6$. While the $4f$ and $5d$ orbitals lie very deep below the vacuum level (≤ 27.8 eV),¹⁶ the Tl⁺- $6s$ and Cl[−]- $3p$ orbital levels lie relatively close to each other (calculated values are¹⁶ -19.8 eV for Tl⁺- $6s$ and¹⁷ roughly -4.00 eV for Cl[−]- $3p$). In the solid, after taking into account the Madelung shift, calculated values show that the Tl⁺- $6s$ level lies near -12.4 eV,¹⁶ and the Cl[−]- $3p$ level lies near -11 eV,¹⁸ even closer to each other. With these in mind it

is conceivable that the electronic valence states of TlCl are strongly influenced by the interaction of Tl⁺- $6s$ and Cl[−]- $3p$ electrons. The overlap of their wave functions therefore contribute significantly to the bonding properties of TlCl solid and thus considerable hybridization of these orbitals can be expected in the valence states of TlCl, and its band structure can be expected to be more complicated than those of alkali halides.

The existence of the $6s^2$ electrons outside of the closed shell of Tl⁺ also makes thallous chloride (thallous bromide also) very different from other CsCl-structured ionic solids. For example, it has a rather small band gap (3.41 eV at 20 °K)¹⁹ for an ionic compound (effective ionic charge $e^* = 8.0e$ in Sziget scale),^{20,21} and both its static and high frequency dielectric constants are usually high ($\epsilon_0 = 37.6$, $\epsilon_\infty = 5.1$),¹⁴ while the difference $\epsilon_0 - \epsilon_\infty$ is also high. Furthermore, thallous halide is the only class of materials known to have negative temperature and pressure coefficients of the static dielectric constant²¹ and negative temperature dependence of Grüneisen parameter.²²

In this paper we report the first uv-photoemission studies on TlCl where the quantum yield and energy-distribution curves (EDC's) of photoemitted electrons were determined for photon energies up to 11.8 eV. The data will be discussed in comparison to the calculated band structure of Overhof *et al.*²³ Also of interest in these studies is the rather strong dependence of EDC's on temperature, which has not been seen in most insulators and semiconductors, but has been seen in silver²⁴ and cuprous²⁵ halides, where the noble-metal nd -orbital levels are close to the halogen

n p -orbital levels.

II. EXPERIMENTAL METHODS

The vacuum chamber and measuring equipment used in these studies have been described in detail previously.¹⁷ The EDC's were measured by the usual ac-modulated retarding potential technique.²⁶ The resolution obtained was about 0.1–0.2 eV. The quantum yields were determined by comparing the photocurrent from the sample with the photocurrent from a calibrated Cs_3Sb phototube.^{17,27} The usual correction was made for the transmission of the LiF window on the vacuum chamber.

Starting thallose chloride material was purchased from Hudson Laboratory (Hudson, Fla.) with ultrahigh purity (99.999%). Thin films of TlCl were sublimed from a quartz crucible onto polished Pt or Mo substrates, which were heat cleaned at 450–475 °C for more than 24 h prior to the sample deposition. The base pressure of the system before sublimation was 1×10^{-10} Torr or lower. During sublimation pressure increased to typically $(1-5) \times 10^{-8}$ Torr. Sample deposition rate was controlled to be extremely low, namely, 3–5 Å/min to avoid pinholes in the thin films.¹⁴ Subsequent x-ray diffraction analyses of the films showed that they were highly, though not completely oriented with the (110) plane of a simple cubic lattice. From the broadening of the x-ray lines, the particle size in the films were calculated²⁸ to be typically 500 Å (assuming negligible strains).

Starting materials and samples were handled under red light. No effects attributable to photolysis have been observed. Films of thickness ranging from 150 to 7500 Å were studied. Except for the photoinjection phenomena observed in the very thin films, which will be discussed in more detail in Sec. IV, no other significant differences were found because of difference in film thickness. More than ten films were studied, the essential features of the data being well reproduced in all cases.

Optical properties of thin films of thallose halides are sensitive to strains due to substrate-sample lattice mismatch. Bachrach and Brown¹⁴ reported observations of exciton peak broadening of about 0.01 eV and peak shift of about the same amount due to strains on TlCl thin films. In our experiments, these were beyond our resolution capability. Also since films of vast range of thickness (150 to 7500 Å) reproduced the essential features of our data, we suggest that the effects of strain in our samples are negligible within our experimental resolution. Otherwise one would expect the EDC's to be thickness dependent because the thicker the films the farther the photoemission

is from the sample-substrate interface.

III. BAND STRUCTURE OF TlCl

In this section we shall briefly discuss the calculated band structure of TlCl so as to provide the readers a general framework in which to view the photoemission data. TlCl crystallizes in simple cubic Bravais lattice with a basis of thallium at (0, 0, 0) and a chlorine at $(\frac{1}{2}, \frac{1}{2}, \frac{1}{2})$. At the time of the writing of this paper there were two theoretical calculations by two different groups on the band structure of TlCl. One was done by Inoue and Okazaki,²⁹ with Heine-Abarenkov model potential method³⁰; the other by Overhof and Treusch²³ with Kohn-Korringa-Rostoker method,³¹ utilizing relativistic ionic potentials. Since both methods yielded similar salient features in the E -vs- \vec{K} diagram, we reproduce in Fig. 1 only one of them (Overhof-Treusch) and shall discuss our data in comparison to it. Among the interesting points about Fig. 1 are (i) the direct gap is at the X point which is the edge of the first Brillouin-zone face. This is strongly contrasted to the other CsCl-structured ionic solids where the direct gaps occur at the zone center Γ ,³² and (ii) the valence bands are about 4 eV wide, much more than the 1.7-eV band width calculated³² for CsI (experimental value is 2.5 eV),³³ the least ionic cesium halide; the highest valence band of TlCl alone is more than 2 eV wide, about four times that of CsI.^{32,33}

Both calculations concluded that the valence bands consists of hybridization of Cl-3 p and Tl-6 s states, and that the lowest conduction band states are Tl-6 p -like. In fact, the strong admixture of Tl-6 s states with Cl-3 p states in the valence bands

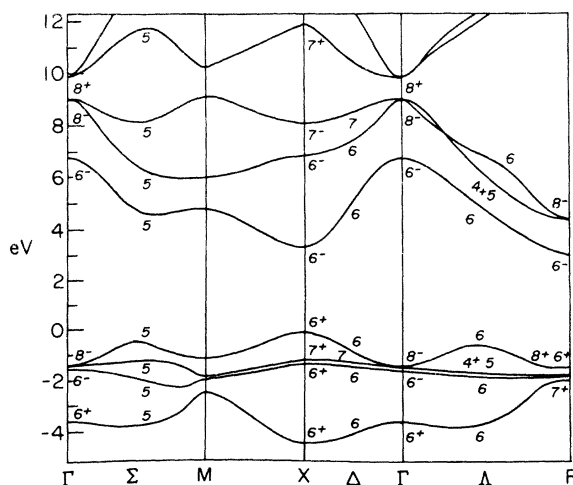


FIG. 1. Band structure of TlCl calculated with KKR method (Ref. 23). Energy scale is plotted taking valence-band maximum as zero.

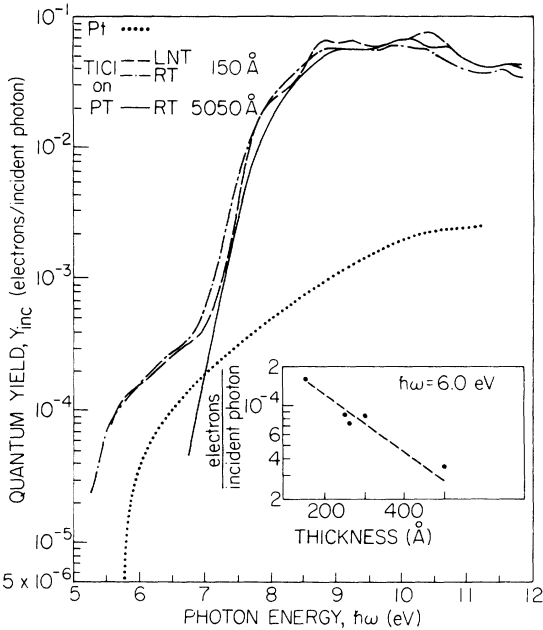


FIG. 2. Quantum yield of TlCl films. The low energy tails in the 150-Å film are due to electrons photoinjected from the substance through the film into vacuum. Dash curve is yield of pure Pt. In the inset is photoinjection yield as a function of TlCl film thickness.

may be the main reason why the valence-band maximum (VBM) occurs at X instead of at Γ . Also, it is probable that the Tl- $6p$ -like states make the conduction band minimum occur at X as compared to the case of CsI where the conduction band minimum is at Γ and the electronic states there are Cs- $6s$ -like.

Figure 1 shows an indirect gap between X_6^+ and R_6^- , about 0.3 eV smaller than the direct gap. This does not exist in the Inoue-Okazaki calculation. However, Overhof and Treusch²³ conceded that the indirect gap might be an artifact of the calculation.

IV. EXPERIMENTAL RESULTS

A. Photoelectric yield

In Fig. 2 we present the quantum yield of TlCl of two different thicknesses. The yields are expressed as Y_{inc} , the number of emitted electrons per incident photon, and are plotted against the incident photon energy.

The tails in the data for the 150-Å film below $h\nu = 7.0$ eV are most likely due to electrons photoinjected into and through the film from the metal substrate as observed by DiStefano and Spicer in CsI.³³ Although it is also possible that they are due to pinholes in the very thin film. Considering the extremely slow evaporation rate in pre-

paring the film to avoid the pinholes, it does not seem very probable. In any case the number of these electrons only amounts to less than $\frac{1}{100}$ of the total yield once the photon energy surpasses the photoemission threshold of TlCl (~ 6.9 eV from Fig. 2). Thus they do not affect the EDC's in the range of $7.5 \leq h\nu \leq 11.8$ eV. In the thicker films the tail disappears.

There are no significant differences between yield data measured at room temperature (RT) and that measured at liquid-nitrogen temperature (LNT). This might lead one to a conclusion that there is no significant change of electronic states of TlCl as temperature changes from RT to LNT. It will, however, become clear in the following discussions that this is not the case. There is no LNT data of the thick (5050-Å) films because at low temperature thick films present severe charging problems that reliable EDC's and yields are hard to measure.

Away from the thresholds the yield data are independent of the film thickness within experimental errors. The yield saturates at about (7–8)% near $h\nu = 10.0$ eV and decreases for $h\nu > 10.0$ eV, in contrast to the case of CsI,³³ in which the photoelectric yield of the thicker film is higher than that of thinner films and increases slowly with photon energy to a value near unity, the enhanced yield in thicker films being due to larger number of phonon scatterings. In TlCl, the decrease of yield for photon energy beyond 10.0 eV is probably due to shorter electron escape depth for higher-energy electrons because of its shorter electron-electron mean free path. The photoelectric threshold determined from the yield data of Fig. 2 is 6.9 ± 0.2 eV. Taking 3.5 eV as the band gap of TlCl at room temperature,¹⁹ the electron affinity is estimated to be 3.4 ± 0.2 eV.

B. Photoinjection

The hot-electron scattering effect in TlCl can be investigated by photoinjecting electrons from the metal substrate through TlCl thin films with photon energy lower than the photoelectric threshold of TlCl as reported by DiStefano and Spicer.³³ In Fig. 2 the low-energy tail below 7.0 eV is assigned to electrons photoinjected from the Pt substrate through the TlCl thin film into vacuum. The thickness dependence of photoinjection yield at $h\nu = 6.0$ eV is shown in the inset of Fig. 2. With Fermi energy at 1.6 eV above the VBM, (determined from Fig. 2) the photoinjected electrons at this photon energy are at $E = 6.9 - 7.6$ eV above the VBM (0–0.7 eV above the vacuum level) of TlCl. A rough fit of $Y_{inj} \propto e^{-T/L}$, where T is the film thickness and L is the hot-electron escape length in TlCl, yields the result $L = 200$ Å for these

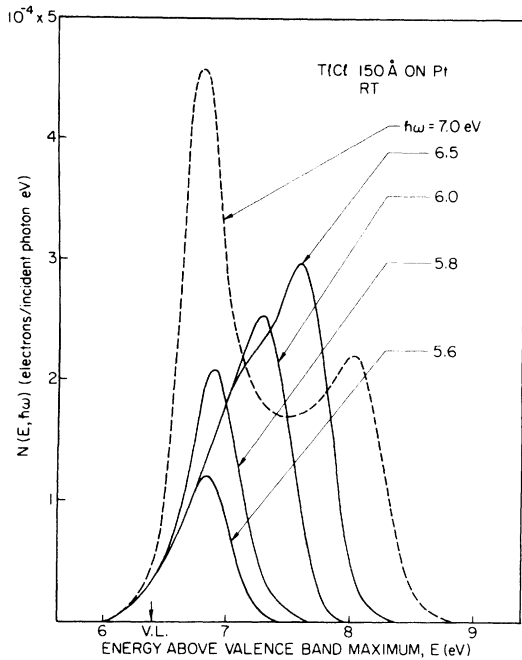


FIG. 3. Energy-distribution curves for electrons photoemitted from a Pt substrate through a TiCl thin film by different photon energies. The 7.0-eV curve consists mostly of electrons from TiCl, which is included in the figure for comparison. The emission is plotted against the final-state energy of the electrons. The arrow in the abscissa denotes vacuum level.

electrons. Since there are only a few data points and the deviation of individual datum from the fitted straight line is large, this number should only be treated as a rough estimate of the average escape depth for electrons of TiCl in the energy

range of 6.9–7.6 eV above the VBM. The TiCl yield is also compared with yields of pure Pt in Fig. 2. In the threshold region, the photoemitted yield is higher than the quantum yield of pure Pt, apparently because the TiCl film lowered the photoemission threshold of Pt by about 0.5 eV.

In Fig. 3 we present the EDC's of the photoemitted electrons from Pt ($\hbar\omega < 7.0$ eV) together with an EDC ($\hbar\omega = 7.0$ eV) containing photoemitted electrons and electrons excited from the valence bands of TiCl. The weaker intensity of emission near the vacuum level in curves for $\hbar\omega = 5.6$ – 6.5 eV as compared to that for $\hbar\omega = 7.0$ eV is partly due to stronger optical absorption in the TiCl film than in the Pt substrate, and partly due to the scattering photoemitted electrons suffered as they traverse the TiCl film. Also note the drop of intensity of the leading peak at $\hbar\omega = 7.0$ eV. This is probably due to the onset of electron-electron scattering near $\hbar\omega = 7.0$ eV (twice the band-gap energy).

C. Energy-distribution curves

EDC's of electrons photoemitted from TiCl with photon energies ranging from 7.8 to 11.8 eV measured at LNT are shown in Fig. 4. These curves have been normalized to the corresponding quantum yield. The number of photoemitted electrons per incident photon are plotted against the initial-state energy of the electrons with the VBM chosen as zero ($E_i = 0$). With increasing photon energy we probe deeper into the valence band and uncover more valence-band density of states. The peak at -1 eV in these EDC's is worth special attention. This peak is very strong up to $\hbar\omega = 10.0$ eV, but then starts to weaken and almost vanishes at

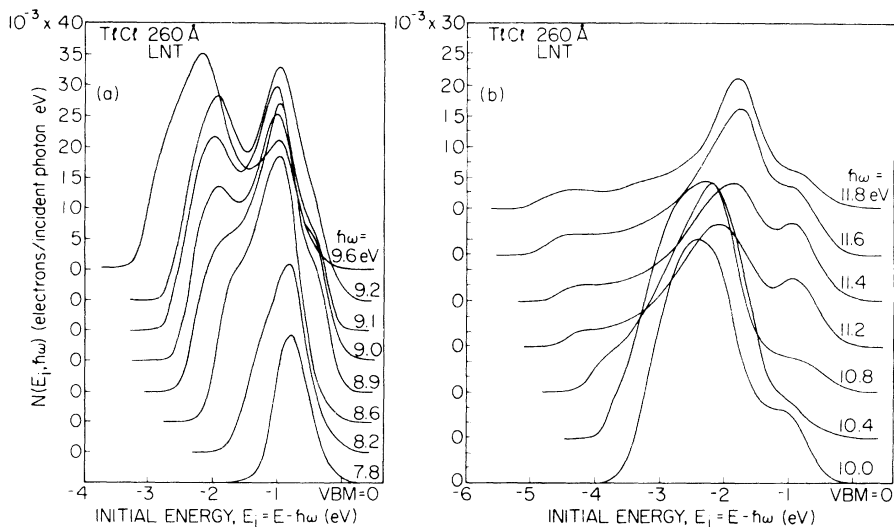


FIG. 4. Energy-distribution curves of photoemitted electrons from TiCl measured at LNT. The emission intensity is plotted against the initial-state energy of the electrons in reference to the valence-band maximum. (a) $7.8 \leq \hbar\omega \leq 9.6$ eV, (b) $10.0 \leq \hbar\omega \leq 11.8$ eV.

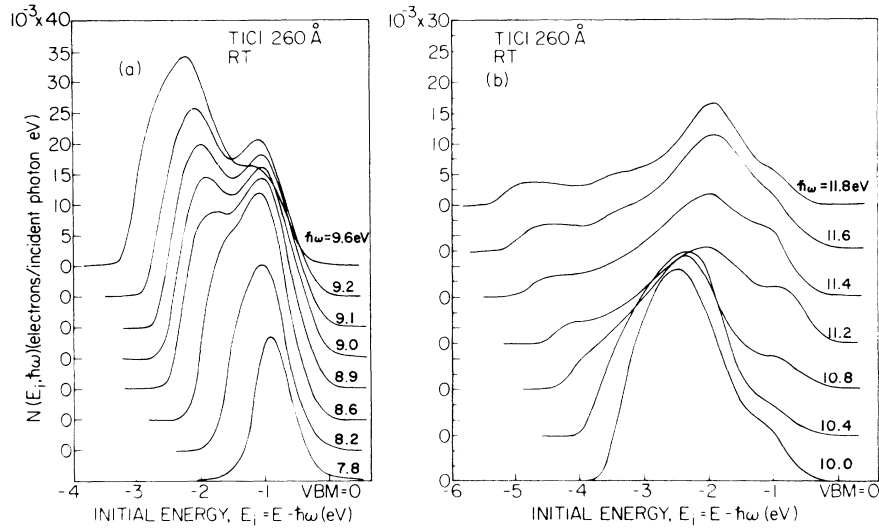


FIG. 5. Energy-distribution curves of photoemitted electrons from TiCl measured at RT. (a) $7.8 \leq \hbar\omega \leq 9.6$ eV, (b) $10.0 \leq \hbar\omega \leq 11.8$ eV.

$\hbar\omega = 10.8$ eV. It reemerges again at 11.2 eV and remains prominent up to 11.8 eV. These features will be discussed in more detail in Sec. V.

In Fig. 5 the EDC's measured at RT for $\hbar\omega < 11.8$ eV are presented. Note that the shoulder near VBM for $8.9 \leq \hbar\omega \leq 9.1$ eV in Fig. 4(a) is now lost in Fig. 5(a). Also note the considerable broadening of peaks compared to the LNT data.

EDC's have also been measured after several thermal cyclings. Each time the results in Figs. 4 and 5 were reproduced, which showed that the changes in the EDC's due to different temperatures were neither accidental nor attributable to any permanent change of the samples due to cooling or warming.

V. DISCUSSIONS

A. Width of the valence bands

In Fig. 6, we present a set of EDC's taken in the maximum energy range available in this work ($\hbar\omega < 12$ eV). The low-energy side of these EDC's is characterized by a break indicated by the arrows at about -4 eV between structure clearly due to primary excitation from the valence band lying above -4 eV, and a region lying below -4 eV which we tentatively assign to inelastically scattered electrons. This separation which gives a valence-band width of 4 eV is similar to that made in³³ CsI and³⁴ CsTe; however, it is made with less certainty here since the bottom of the band (as we assign it) only clears the potential barrier at the surface by about 1.5 eV; whereas, in CsI and CsTe the clearance is significantly larger. Clearly, additional measurements at

higher $\hbar\omega$ should be made to further test our assignment of the band width. However, it should be noted that it is in agreement with band calculation^{23,29} (see Fig. 8).

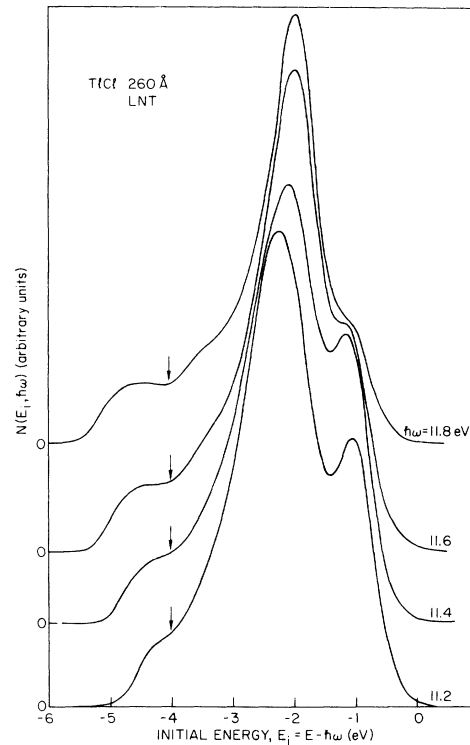


FIG. 6. Energy-distribution curves of photoemitted electrons from TiCl measured at LNT. The arrows denote the extent of the valence-band width. Structure to the left of the arrows are due to scattered electrons.

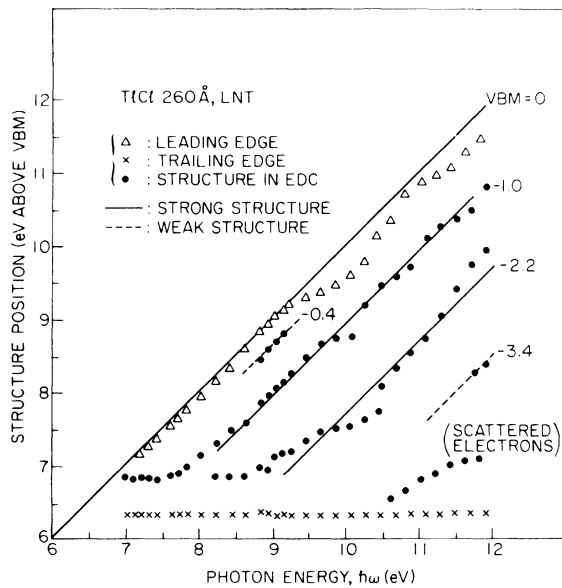


FIG. 7. Structure plot for EDCs of TiCl measured at LNT. Solid 45° lines through structure points denote strong density of states, dashed line denotes weak structure in density of states.

B. Electronic structure

Important information contained in the EDC's in Fig. 4 can be succinctly and instructively expressed in the structure plot shown in Fig. 7, where the final energy of pieces of structure in the EDC's have been plotted against incident photon energy. Structure in the valence-band density of states will then manifest itself by structure in the EDC's that moves along a 45° line in the structure plot as photon energy increases, whereas structure in the conduction-band density of states will show up as a horizontal line.

From Fig. 7 we see that there are two pieces of strong density of states in the valence bands, located at about 1.0 and 2.2 eV, respectively, below the VBM, and two additional pieces of weak structure at -0.3 and -3.4 eV. The lowest-lying structure in the structure plot is attributed to scattered electrons as discussed above. The fact that the structure in the EDC's either deviate somewhat from 45° lines (structure at -1.0 and -2.2 eV) or appear only within a very narrow range of photon energy (structure at -0.3 and -3.4 eV) is suggestive of \vec{k} conservation or other optical selection rules in TiCl. Further evidence supporting the importance of \vec{k} conservation comes from the fact that as we trace across the structure plot the leading edge of the EDC's does not follow exactly a 45° line either. Note that even in the case where \vec{k} conservation is important, a strong valence-band density of state peak still follows roughly

a 45° line in the structure plot over a large $\hbar\omega$ range.³⁵

The structure at -0.3 eV appears as a weak shoulder in the photon energy range $8.8 \leq \hbar\omega \leq 9.1$ eV. It probably is due to direct transitions from near the valence-band maximum. As such, it indicates conduction-band structure (in the vicinity of \vec{k} space of the VBM) located 8.5–8.8 eV above the VBM. This, of course, does not imply a peak in the density of states since the structure appears over such a small $\hbar\omega$ range.³⁶

As for the -3.4 -eV structure, it begins to appear at $\hbar\omega = 11.6$ eV. It is possible that it may grow further with $\hbar\omega > 11.8$ eV due to increasing matrix elements. An assignment of this structure to structure in the valence-band density of state would give a fair agreement with the calculated band structure, as will be shown in the following discussion. In any event, obtaining EDC's for higher photon energies will be valuable to test this assignment.

The fact that for $9.3 \leq \hbar\omega \leq 10.6$ eV the leading edge falls below the Einstein limit (indicated by VBM=0) suggests a lack of final states with \vec{k} vectors near that of the valence-band maximum for final states 9.3 to 10.6 eV above the VBM (see Fig. 1). The Einstein limit is defined by the expression $E_{\text{final}} = E_{\text{VBM}} + \hbar\omega$, where E_{final} is the maximal final-state energy and E_{VBM} is the energy of the VBM.

To relate as well as possible the photoemission data to the calculated-band structure, we compare the structure plot (Fig. 10) and the EDC's (Fig. 7) to the valence-band density of state³⁷ (Fig. 8) derived from the calculated E -vs- \vec{k} diagram (Fig. 2). We see that in addition to the band width there is fair qualitative agreement between the experimental data and the calculated results in that the number of density-of-state peaks is the same. However, quantitatively the agreement is

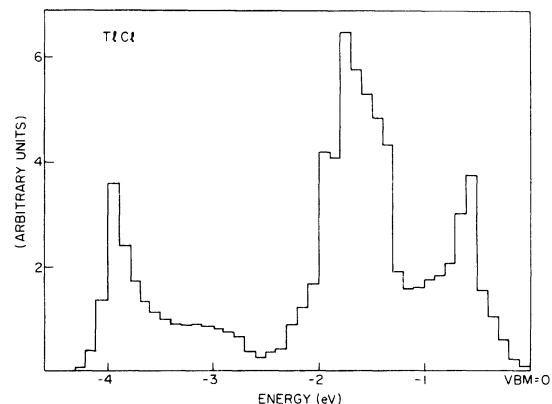


FIG. 8. Valence-band density of state derived from Fig. 2 (Ref. 37).

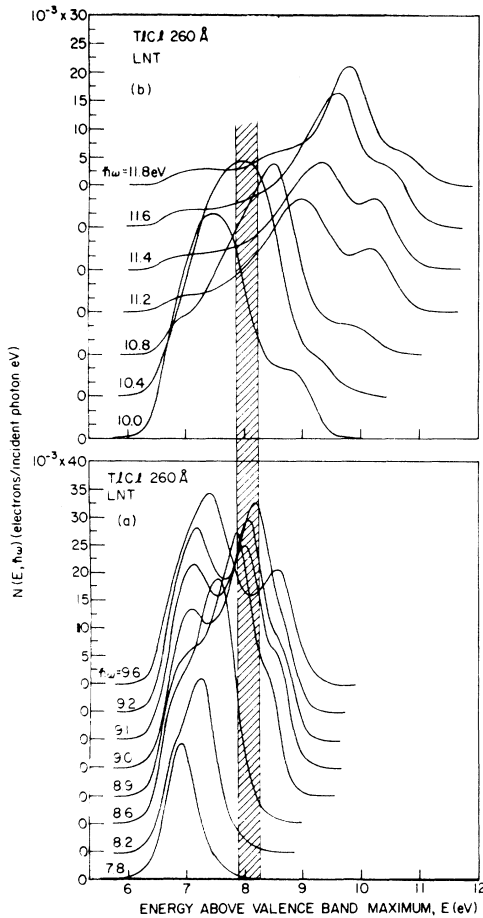


FIG. 9. Same curves from Fig. 4, plotted against the final-state energy of the photoemitted electrons. The shaded area denotes strong conduction-band density of state.

not satisfactory. For example, the first two calculated density-of-state peaks have to be shifted by 0.5 eV down the energy scale in order to confirm to the experimental data. Also, the third peak in the calculated density-of-states lies about 0.5 eV deeper as compared to the experimental results.

To check the correspondence of the calculated conduction band to the photoemission experiments, we redraw the curves of Fig. 4 in Fig. 9 with the final-state energy of photoemitted electrons as the x axis. Both peaks originated from -1.0 and -2.2 eV are very strong near final-state energy 8.1 eV and both suffer sudden drop of intensity as they move to higher final-state energy. This is suggestive of a strong conduction density of state near 8.1 eV above the VBM. Returning to Fig. 2, it could correspond to the flat-band regions near the X points and in the Σ directions near 8.2 eV. The peak originated from -1.0 eV almost van-

ishes when it is in the final-state energy region 9.0–10.0 eV. This is indicative of a minimal density-of-state area between 9.0 and 10.0 eV above the VBM, in agreement with the 0.8 eV gap between the third and the fourth conduction bands (from 9.2 to 10.0 eV) in the calculated band structure (Fig. 2).

C. Temperature effects on EDC'S

Much less has been done in studying solids using ultraviolet photoemission spectroscopy below room temperature than at room temperature. This is due to the fact that the experimental resolution (typically 0.1 to 0.2 eV) is usually larger compared to kT at room temperature (0.025 eV). Thus, unless unusually strong coupling between the lattice and electronic structure is present, cooling to, for example, 77°K ($kT = 0.007$ eV), would not be expected to strongly affect the EDC's. This expectation has generally been found in such diverse materials as the columns³⁸ IV and³⁹ III–V photoemitters, transition metal oxides,⁴⁰ and metals.⁴¹ However, a systematic study of photoemission at low temperatures has not been made in all materials.

In contrast to most other studies, Bauer and Spicer found extreme temperature dependence in the silver halides²⁴ (e.g., change in the width of structure of order 0.3 eV on cooling from 300 to 77°K, $\Delta kT = 0.018$ eV). This extreme temperature dependence is also reflected in the optical data from the silver halides.⁴² Bauer and Spicer²⁴ suggested that the temperature dependence was due to a strong modulation of the overlap between the halogen p and silver d valence electrons due to the large change in vibrational amplitude in cooling

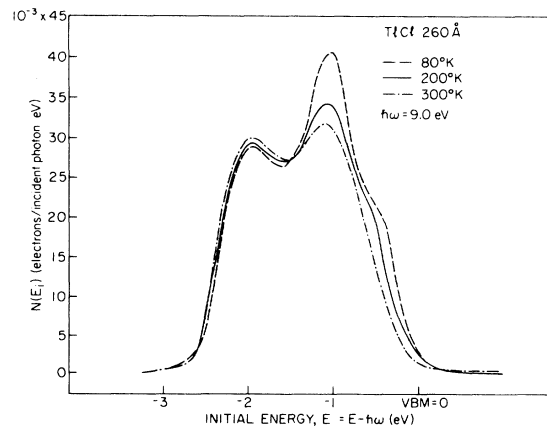


FIG. 10. Energy distribution curves of photoemitted electrons from TiCl₃ for $\hbar\omega = 9.0$ eV measured at three different temperatures. Note the sharpening of the -1.0 -eV peak and the emergence of the -0.3 -eV shoulder.

from 300 to 77 °K. The somewhat clumsy term "dynamic modulation of orbital hybridization of electronic states" has been used to describe this effect. In order to test this suggestion temperature-dependent studies of the Cl and Tl halides were undertaken. In the first case Cu-*d* and halogen-*P* and in the second Tl-*s* and halogen-*P* overlap occurs in the valence band; therefore, strong temperature dependence of the EDC's would also be expected if the Bauer-Spicer suggestion was correct. As will be reported here, such dependence has been found in TlCl, although they are not as strong as in the silver halides. As reported elsewhere,⁴³ it has also been found in the copper halides.

Anomalously large dependence of EDC's on temperature is typified in Fig. 10 by comparing EDC's measured at three different temperatures for $\hbar\omega = 9.0$ eV. Not only the peaks sharpen greatly but also new pieces of structure emerge when the temperature is decreased from 300 to 80 °K. As suggested by Bauer and Spicer,⁴⁴ this strong temperature dependence of EDC's can be seen among the class of materials in which (i) valence-band wave functions are moderately localized, (ii) valence-band wave functions are combinations of two ionic (or atomic) orbitals whose ionic (or atomic) energy levels are fairly close to each other, especially after Madelung energy correction in the solids, and (iii) Debye temperatures Θ lies within the range of experimental temperature variation.

Rubloff *et al.*,⁴⁵ in explaining the large temperature effect on reflectance of some alkali halides, suggested that the above mechanism may be plausible for the conduction-band states as well.

In the case of thallos chloride, the valence-band states have been shown to be a strong hybridization of Tl⁺-6*s* and Cl⁻-3*p* orbitals^{23,29}; the ionic energy levels of Tl⁺-6*s* and Cl⁻-3*p* have been calculated to be only about 1.6 eV apart after Madelung energy adjustments¹⁶⁻¹⁸; the Debye temperature is somewhere between 126 and 140 °K,^{46,47} well within the temperature range of our experiment (77-300 °K); and the partly covalent, partly ionic properties of TlCl suggest that the valence state wave functions are moderately localized. Thus it is not surprising to see the strong temperature dependence of EDC's in TlCl.

To first approximation the temperature effects on the electronic states of TlCl can be explained as follows: When the temperature of TlCl changes, a static change and a dynamic change happen to the crystal. The static change is the thermal expansion (or contraction) of the lattice; the dynamic change is the increase (or decrease) of the amplitude of lattice vibration. The thermal expansion

or contraction of the lattice alters the ionic spacings, which in turn alter the Madelung energy and the orbital hybridization of the electronic states. The change of vibration amplitude of lattice alters the extent to which the lattice spacings fluctuate. The fluctuating ionic spacings modulate the orbital hybridization but tend not to affect the Madelung energy, since Madelung energy comes from the long-range electrostatic interaction, any change of local contributions tends to average out when the sum is taken. On the other hand, the orbital hybridization being short-range interaction in nature, its fluctuation due to fluctuation of ionic spacings will not be averaged out, and will contribute to the broadening of energy levels. Thus the static effects of temperature on energy levels arise both from change of orbital hybridization and change of Madelung energy, and cause the shift of energy levels. The dynamic effects, however, arise mainly from change of fluctuation of orbital hybridization, and, we suggest, cause the broadening of energy levels.

In Fig. 10, the peak position shift (=0.02 eV) is much smaller than the broadening of the peak (taken at 90% peak height, is =0.2 eV) when sample temperature is increased from 80 to 300 °K. This is understandable from the following considerations: The average mean-square amplitude of lattice vibration as given by Debye-Waller theory⁴⁸ is

$$\chi^2 = \frac{3\hbar^2 T^2}{MK_B \Theta_D^3} \int_0^{\Theta_D/T} \left(\frac{1}{2} + \frac{1}{e^z - 1} \right) z dz, \quad (1)$$

where \bar{M} is the average mass of Tl⁺ and Cl⁻ ions.^{17,49} From this we obtain the average root-mean-square amplitude as

$$X(T) \approx 2 \times (0) (T/\Theta_D)^{1/2} \text{ for } T \gg \frac{1}{2}\Theta_D, \quad (2)$$

where $X(0)$ is the average root-mean-square amplitude at $T = 0$ °K. Under this approximation, as sample temperature varies from 80 to 3000 °K, the vibration amplitude changes by

$$\frac{X(300 \text{ °K}) - X(80 \text{ °K})}{X(80 \text{ °K})} \approx 93.7\%, \quad (3)$$

i.e., from 0.131 to 0.253 Å. On the other hand, the average linear thermal expansion coefficient of TlCl in the temperature range of 80-300 °K is about 5×10^{-5} °K⁻¹,²² which causes ionic spacing to change by 1.1% as temperature varies from 80 to 300 °K. Consequently the static thermal expansion does not affect the electronic states as strongly as the change of lattice vibration amplitude does.

Since the lattice vibrations, i.e., phonons, exert strong influence on the electronic states of TlCl through fluctuations of orbital hybridization, we

can expect the orbital hybridization of electronic states to have strong effects on the vibrational spectrum of TlCl. One may need to take this into account for a better understanding of the lattice dynamics of this material.

Lattice dynamics of CsCl-structured ionic crystals, i.e., CsCl, CsBr, and CsI have been successfully calculated theoretically⁵⁰ with simple shell model.⁵¹ Unfortunately, the same cannot be said of TlCl,⁵² or TlBr, or the Ag and Cu halides.⁵³ Both rigid ion models and simple shell models gave poor description of the phonon dispersion curves. Cowley and Okzaki¹⁵ resorted to a shell model with as many as 14 parameters and still encountered discrepancies with experimental results of TlCl. The reason for the success with Cs halides and failure with TlCl in this matter may lie in the fact that bonding in CsCl is almost purely ionic with the valence electronic states unhybridization with Cs states while in TlCl the hybridization occurs between the Tl and Cl valence electronic states (although there may be hybridization in the conduction band states in Cs halides). Lattice vibration would induce change in the valence electronic states which would in turn change the bonding strength. This makes the harmonic approximation employed in the rigid ion models and shell models highly inappropriate. We suggest that with this taken into account, many thermodynamic properties of TlCl (and TlBr), including Grüneisen parameter, dielectric constants and phonon dispersion curves, may be understood better. The same arguments can be made for the lattice spectra of the silver and copper halides.⁵⁴

In essence for both optical excitation and lattice dynamics, the electron-lattice interaction is so strong that it cannot be treated as a perturbation in the Hamiltonian of the electron-lattice system. A usual perturbation treatment in the formalism of electron-phonon interaction would give the broadening of the EDC structure in the order of $k_B \Delta T$, which is roughly 0.02 eV as temperature increases from 80 to 300 °K. This value is an order of magnitude smaller as compared to the experimentally observed broadening in Fig. 10. Therefore, a many-body formalism seems to be demanded for this problem.

D. Chlorination of TlCl

It may also be worth mentioning here that Tuthasi¹³ reported a conversion of TlCl to Tl₂Cl₃ by exposing TlCl thin films to Cl₂ gas of 1–10 Torr for 10 min. In an effort to observe the effects of decreasing number of Tl⁺ – 6s electrons as TlCl is converted into Tl₂Cl₃, we have tried exposing TlCl thin films to Cl₂ gas up to 500 lang-

muir (1 L = 10⁻⁶ Torr sec) at 10⁻⁸ Torr through a leak valve to the photoemission chamber. However, no significant differences were observed in the EDC's before and after Cl₂ exposure. We have also tried exposure at 50 °C (TlCl thin films sublime readily for $T > 50$ °C) and no effects were found. Since the equipment forbids higher concentration of Cl₂, we have not tried exposure at higher langmuir rate.

VI. CONCLUSIONS

In conclusion, photoemission measurements have been used to determine important features in the band structure of TlCl. A valence-band width of 4.0 eV has been estimated. Evidence has been found for two strong valence-band density of state, locating at -1.0 and -2.2 eV (with respect to the VBM), respectively, and weaker structure has been located at -3.4 eV. Also deduced from the EDC's are a large conduction-band density of states near 8.1 eV and a minimal density-of-state region from 9.0 to 10.0 eV. The \vec{k} conservation rule was found to be important in the optical transitions in TlCl. Theoretically calculated band structure compares well with the photoemission data qualitatively but not quantitatively in several aspects.

Hot-electron scattering effects have been investigated by photoinjecting electrons from the Pt substrate through TlCl thin films into vacuum with photon energy less than the photoelectric threshold of TlCl. By a rough exponential fit to the photoinjection yield as a function of film thickness, the electron escape length has been found to be ≈ 200 Å for electrons 6.9–7.6 eV above the VBM (0–0.7 eV above the photoelectric threshold).

Relatively strong temperature dependence of TlCl EDC's has been found, as in the case of Ag and Cu halides. All of these three classes of materials are characterized by valence-bands containing strong hybridization between valence states on the cations and the anions. Likewise, the conventional rigid ion or simple shell model has proven inadequate to predict the dispersion curves lattice vibration for these materials. We suggest that these results are due to the same phenomena: A very strong coupling between the lattice and the electronic states which results from the anion-cation valence hybridization being dynamically modified on a nearest neighbor scale by lattice vibration.

It is recognized that in regard to electron-lattice interaction it would be interesting to examine the problems in the high T_c superconductors where strong coupling between lattice and electronic states may be so important.

ACKNOWLEDGMENTS

The authors wish to express their gratitude to Dr. H. Overhof for supplying the results of cal-

culated TiCl valence-band density of states and their appreciation to Dr. F. C. Brown, Dr. R. S. Bauer, and Dr. T. H. Geballe for helpful conversations.

- †Work supported in part by NASA and by NSF through the Center for Materials Research at Stanford University and by U. S. Army Research Office-Durham.
- ¹K. Kodama, S. Saito, and S. Minomura, *J. Phys. Soc. Jpn.* **33**, 130 (1971).
- ²J. W. Hodby, A. Bonders, F. C. Brown, and S. Foner, *Phys. Rev. Lett.* **19**, 952 (1967).
- ³H. Tamura, T. Masumi, and K. Kobayashi, *J. Phys. Soc. Jpn.* **23**, 1173 (1967); J. W. Hodby, G. T. Jenkin, K. Kobayashi, and H. Tamura, *Solid State Commun.* **10**, 1017 (1972).
- ⁴D. Fröhlich, B. Staginnus, and S. Thurm, *Phys. Status Solidi* **40**, 287 (1970).
- ⁵Y. Onodera, *Opt. Commun.* **3**, 113 (1971).
- ⁶S. Kurita and K. Kobayashi, *J. Phys. Soc. Jpn.* **26**, 1557 (1967).
- ⁷S. Kurita and K. Kobayashi, *J. Phys. Soc. Jpn.* **28**, 1096 (1970).
- ⁸O. Aita, I. Nagakura, and T. Sagawa, *J. Phys. Soc. Jpn.* **30**, 1414 (1971).
- ⁹S. Saito, M. Watanabe, Y. Iguchi, S. Nakai, Y. Nakamura, and T. Sagawa, *J. Phys. Soc. Jpn.* **33**, 1638 (1972).
- ¹⁰A. M.-E. Saar and M. A. Elango, *Sov. Phys.-Solid State* **13**, 2985 (1972).
- ¹¹O. Aita, I. Nogakura, and T. Sagawa, *J. Phys. Soc. Jpn.* **33**, 750 (1972).
- ¹²H. Zinngrebe, *Z. Phys.* **154**, 495 (1959).
- ¹³S. Tutihasi, *J. Phys. Chem. Solids* **12**, 344 (1959).
- ¹⁴R. Z. Bachrach and F. C. Brown, *Phys. Rev. B* **1**, 818 (1970).
- ¹⁵E. R. Cowley and A. Okazaki, *Proc. R. Soc. A* **300**, 45 (1967).
- ¹⁶J. Overton and J. P. Hernandez, *Phys. Rev. B* **7**, 778 (1973).
- ¹⁷R. S. Bauer, Ph.D. dissertation (Stanford University, 1970) (unpublished) (Xerox University Microfilms No. 71-19646); R. S. Bauer and W. E. Spicer, second preceding paper, *Phys. Rev. B* **14**, 4539 (1976).
- ¹⁸In Ref. 16, the Br⁻-4*p* free ionic level has been shown to shift down by about 7 eV because of the Madelung energy in the solid. We believe this value is also adequate for the Cl⁻-3*p* level since TiCl and TiBr crystallize in the same structure with roughly the same lattice constants.
- ¹⁹D. Forhlich, J. Treusch, and W. Kottler, *Phys. Rev. Lett.* **29**, 1603 (1972).
- ²⁰G. O. Jones, D. H. Martin, P. A. Mawer, and C. H. Perry, *Proc. R. Soc. A* **261**, 10 (1961).
- ²¹G. A. Samara, *Phys. Rev.* **165**, 959 (1968).
- ²²A. D. Redmond and B. Yates, *J. Phys. C* **5**, 1589 (1972).
- ²³H. Overhof and J. Truesch, *Solid State Commun.* **9**, 53 (1971).
- ²⁴R. S. Bauer and W. E. Spicer, *Phys. Rev. Lett.* **25**, 1283 (1970). R. S. Bauer, S. F. Lin, and W. E. Spicer, third preceding paper, *Phys. Rev. B* **14**, 4527 (1976).
- ²⁵S. F. Lin, R. S. Bauer, W. F. Krolikowski, and W. E. Spicer, *Bull. Am. Phys. Soc.* **17**, 143 (1972).
- ²⁶W. E. Spicer and C. N. Berglund, *Rev. Sci. Instrum.* **35**, 1665 (1964); R. C. Eden, *ibid.* **41**, 252 (1970).
- ²⁷R. Y. Koyama, Ph.D. dissertation (Stanford University, 1960) (unpublished).
- ²⁸H. P. Klug and L. E. Alexander, *X-Ray Diffraction Procedures* (Wiley, New York, 1954), p. 494.
- ²⁹M. Inoue and M. Okazaki, *J. Phys. Soc. Jpn.* **31**, 1313 (1971).
- ³⁰V. Heine and I. V. Abarenkov, *Philos. Mag.* **9**, 451 (1924); I. V. Abarenkov and V. Heine, *ibid.* **12**, 529 (1965); A. O. E. Aninalu and V. Haine, *ibid.* **12**, 1249 (1965).
- ³¹J. Korrynga, *Physica (Utr.)* **13**, 392 (1947); W. Kohn and N. Rostoker, *Phys. Rev.* **94**, 1111 (1954); F. S. Ham and B. Segall, *ibid.* **124**, 1786 (1961).
- ³²Y. Onodera, *J. Phys. Soc. Jpn.* **25**, 469 (1968); U. Rossler, *Phys. Status Solidi* **34**, 207 (1969).
- ³³T. H. DiStefano and W. E. Spicer, *Phys. Rev. B* **7**, 1554 (1973).
- ³⁴R. A. Powell, W. E. Spicer, G. B. Fisher, and P. Gregory, *Phys. Rev. B* **8**, 3987 (1973).
- ³⁵W. E. Spicer, *Electronic Density of States*, edited by L. H. Bennett (U. S. GPO, Washington, D.C., 1971), SD Catalog No. C 13:323, p. 139.
- ³⁶W. E. Spicer, *J. Phys. (Paris)* **34**, C6-19 (1973).
- ³⁷H. Overhof (private communication).
- ³⁸T. M. Donovan, Ph.D. dissertation (Stanford University, 1970) (unpublished).
- ³⁹A. D. Baer (private communication).
- ⁴⁰G. F. Derbenwick, Ph.D. dissertation (Stanford University, 1970) (unpublished).
- ⁴¹K. Yu (private communication).
- ⁴²N. J. Carrera and F. C. Brown, *Phys. Rev. B* **4**, 3651 (1971).
- ⁴³S. F. Lin, W. E. Spicer, and R. S. Bauer, preceding paper, *Phys. Rev. B* **14**, 4551 (1976).
- ⁴⁴R. S. Bauer and W. E. Spicer, *Electron Spectroscopy*, edited by D. A. Shirley (North-Holland, Amsterdam, 1972), p. 569.
- ⁴⁵G. W. Rubloff, J. Freeouf, H. Fritzsche, and K. Murase, *Phys. Rev. Lett.* **26**, 1317 (1971).
- ⁴⁶The authors of Ref. 1, using room-temperature value of elastic constants, calculated $H_d = 126.1^\circ\text{K}$ for TiCl; while authors of Ref. 22 calculated $H_d = 140^\circ\text{K}$ for TiCl using low-temperature elastic constants data of Ref. 36.
- ⁴⁷T. Vallin, K. Marklund, and J. O. Silestrom, *Ark. Fys.* **32**, 515 (1966).
- ⁴⁸J. M. Ziman, *Theory of Solids* (Cambridge U.P., London, 1969), p. 60.
- ⁴⁹R. W. James and E. M. Firth, *Proc. R. Soc. Lond. A* **117**, 62 (1927).
- ⁵⁰A. A. Z. Ahmad, H. G. Smith, N. Wakabayashi, and M. K. Wilkinson, *Phys. Rev. B* **6**, 3956 (1972).
- ⁵¹A. D. B. Woods, W. Cochran, and B. N. Brockhouse, *Phys. Rev.* **119**, 980 (1960).

⁵²C. Carabatos, B. Hennion, K. Kunc, F. Moussa, and
C. Schwab, Phys. Rev. Lett. 26, 770 (1971).

⁵³P. R. Vijayaraghavan, R. M. Nickkow, H. G. Smith,

and M. K. Wilkinson, Phys. Rev. B 1, 4819 (1970).

⁵⁴R. S. Bauer (private communications). See Sec. V C of
Ref. 24.